



ELSEVIER

Available online at www.sciencedirect.com

SCIENCE @ DIRECT®

Journal of Computational and Applied Mathematics 177 (2005) 401–425

JOURNAL OF
COMPUTATIONAL AND
APPLIED MATHEMATICS

www.elsevier.com/locate/cam

Honeycomb and k -fold Hermite subdivision schemes

Yonggang Xue, Thomas P.-Y. Yu*

Department of Mathematical Sciences, Rensselaer Polytechnic Institute, Troy, NY 12180-3590, USA

Received 15 April 2004

Abstract

We construct Hermite subdivision schemes for hexagon tiling and quadrisection $/\sqrt{3}$ refinement, which have applications in free-form surface design. Such subdivision schemes operate in such a way that when a “jet” of Hermite data is attached to each of the *vertices* in a coarse hexagon tiling, the subdivision rule is capable of defining Hermite data attached to the *vertices* of successively refined hexagon tilings, in such a way that the data converges to a smooth limit function which has Hermite data consistent with that generated by the subdivision process. Such a “vertex-based scheme on hexagon tiling” can be thought of as a “face-based schemes on triangular tiling”. This simple connection allows us to put the construction under the mathematical framework of subdivision operators and refinement equations.

Along the way, we introduce a general concept called *k-fold Hermite subdivision*, and analyze its properties with the help of the strong convergence theory of refinement equation. The case of $k = 2$, together with an appropriate symmetry condition, can be used to handle the construction of honeycomb Hermite subdivision schemes. In particular, our framework allows us to construct smoother versions of two interesting honeycomb subdivision schemes in the literature.

© 2004 Elsevier B.V. All rights reserved.

MSC: 41A05; 41A15; 41A63; 42C40; 65T60; 65F15

Keywords: Refinable function; Vector refinability; Subdivision scheme; Hermite subdivision scheme; Shift invariant subspace; Symmetry; Smoothness; Subdivision surface; Tiling; Honeycomb

* Corresponding author.

E-mail addresses: xuey@rpi.edu (Y. Xue), yut@rpi.edu (T.P.-Y. Yu).

1. Introduction

In [8–10], the authors introduce a class of subdivision schemes such that when a “jet” of Hermite data is attached to each of the vertices in a coarse scale tiling, the subdivision rule is capable of defining Hermite data attached to the *vertices* of successively refined tilings, in such a way that the data converges to a smooth limit function f which has Hermite data consistent with that generated by the subdivision process.

The four tiling and refinement rules shown in Figs. 1(a)–(d) are considered in the articles [9,10], for the interpolatory case and the non-interpolatory (a.k.a. approximating) case, respectively. The article [8] deals with the cases of (a') and (b'). One of the main goals of this article is to deal with the construction in the cases of (c') and (d'). As we shall see, a major difference between the hexagon ((c') & (d')) and square ((a') & (b')) tiling cases is that the former involves subdivision operators with *twice* the multiplicity of those in the latter case.

Such subdivision schemes have direct application to surface modelling, see [14,15] and the references therein. We refer also to the articles [9,10] for the motivation of using Hermite subdivision schemes in free-form surface modelling.

We note that each of the tilings in each of the panels Figs. 1(a)–(d) is *dual* (in the graph-theoretic sense) to the corresponding one in the panel below. This means that if we take the tiling and refinement rule in, say (a), and think of constructing subdivision schemes based on attaching data to the *centers of faces*, instead of to the vertices, then the resulted subdivision scheme is effectively one based on the tiling and refinement rule in (a'). In other words, a “face-based scheme” (see [8]) based on the tiling and refinement depicted in each panel is the same as a “vertex-based scheme” based on the tiling and refinement in the panel directly above/below, and vice versa.

As the dual of a triangle tiling is a hexagon tiling, a subdivision scheme based on associating data to the *vertices* of (successively refined) hexagon tilings can be regarded as a subdivision scheme based

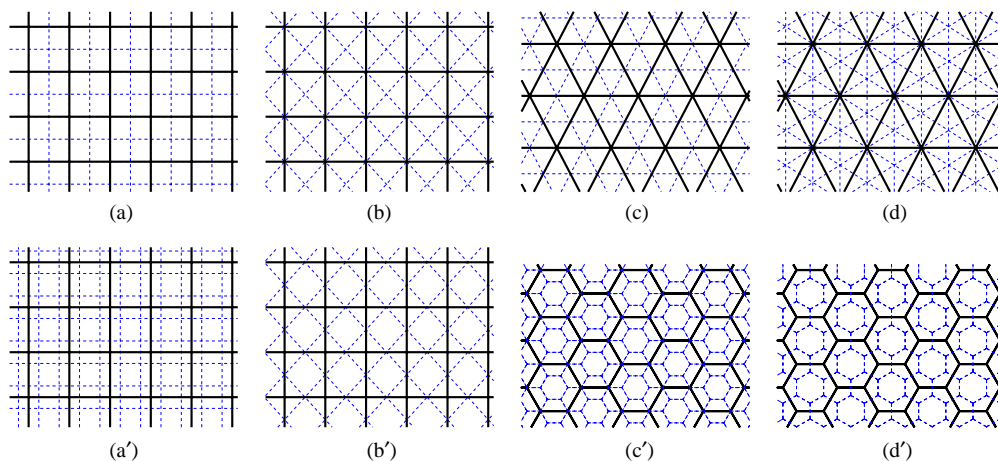


Fig. 1. 2D topological refinement schemes based on the square, triangle and hexagon tiling. Two different refinement rules are shown for each of the three tilings. The black solid lines show the tiling at scale 0, the blue dashed lines show the tiling at scale 1; note that the scale 0 and scale 1 tilings are similar, so the same refinement can be continued to scale 2,3,... (For the colour version of this figure the reader is referred to the web version of this article at doi:10.1016/j.cam.2004.09.056).

on associating data to the *faces* of (successively refined) triangle tilings. The equivalence of these two viewpoints is important for our purposes for the following reasons:

- Subdivision schemes directly based on the *former* point of view—referred to as *honeycomb subdivision schemes*—have been proposed in [2,3].
- A subdivision scheme based on the *latter* point of view can be quite easily rewritten in the form of a subdivision operator (2.3), allowing us to utilize the extensive results available for analysis and construction. In particular we will use this approach to construct what we later call honeycomb Hermite subdivision schemes.

We shall spell out the connection of these two viewpoints in some details in Section 2. Such a connection is also stated (somewhat implicitly) in the article [12].

Organization: In Section 2, we first review two different honeycomb subdivision schemes. In Section 2.1, we illustrate how each of these honeycomb subdivision schemes can be cast as what is usually called a subdivision operator in the wavelet literature; the latter, in turn, is directly connected to a so-called refinement equation. Thanks to such connections, the extensive knowledge of refinement equation is at our disposal for studying—and generalizing—honeycomb subdivision schemes.

In Section 3, we define and analyze a general notion of *k-fold Hermite subdivision schemes*, and study their sum-rule and approximation order properties. In Section 4, we study *symmetric honeycomb Hermite subdivision schemes*, which, on the one hand, can be viewed as a generalization of honeycomb subdivision schemes as those presented in [2,3] and, on the other hand, is a special case of two-fold Hermite subdivision schemes defined in Section 3. We shall derive the *symmetry* conditions for honeycomb Hermite subdivision schemes. In Section 5 we shall combine the general results with computational tools to construct specific examples of symmetric honeycomb Hermite subdivision schemes. Section 6 concludes the article and address some subtle issues and open questions. The Appendix section, contains the proofs of the two major theorems in this article.

Notations: Let $\ell(K) := \{v : K \rightarrow \mathbb{R}\}$ and $[\ell(K)]^{m \times n} := \{v : K \rightarrow \mathbb{R}^{m \times n}\}$ be equipped with the obvious vector space structures. The Banach spaces $\ell^p(K)$ and $[\ell^p(K)]^{m \times n}$, $p \in [1, \infty]$, are defined in the usual way (after we equip K with the counting measure); $\ell^0(K)$ (resp. $[\ell^0(K)]^{m \times n}$) denotes the subspace of $\ell(K)$ (resp. $[\ell(K)]^{m \times n}$) of finitely supported sequences.

In this paper, A_r is the (ordered) set of s -tuples (with $s = 2$ in most cases) of non-negative integers with sum no greater than r , ordered by the lexicographic ordering. $\mathcal{S}(E, A_r)$ is the $\#A_r \times \#A_r$ matrix that measures how Hermite data of a bivariate function changes upon a linear change of variable by $E \in \mathbb{R}^{s \times s}$: if

$$\partial^{\leq r} f(x) := [D^v f(x)]_{v \in A_r} \in \mathbb{R}^{1 \times \#A_r}, \tag{1.1}$$

then

$$f \in C^r(\mathbb{R}^2), \quad g = f(E \cdot) \implies \partial^{\leq r} g = \partial^{\leq r} f(E \cdot) \mathcal{S}(E, A_r). \tag{1.2}$$

An *isotropic dilation matrix*, or just dilation matrix, M is an $s \times s$ matrix with integer entries which is similar to a diagonal matrix with diagonal entries of a constant modulus $\sigma > 1$.

When a dilation matrix M is clear for the context, we define the notation

$$D_n^{\leq r} f(x) := \partial^{\leq r} f(x) \mathcal{S}(M^{-n}, A_r) \in \mathbb{R}^{1 \times \#A_r}. \tag{1.3}$$

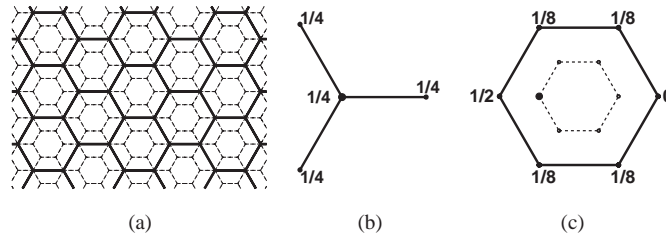


Fig. 2. (a) Hexagon tiling and a refinement; (b) and (c) A half box-spline subdivision rules [2]: old vertex rule ((b)), new vertex rule ((c)).

The vector on the right-hand side consists precisely of all the mixed directional derivatives of f of order upto r at the point x and in directions $M^{-n}e_j, j = 1, \dots, s$.

Since it is easy to distinguish from the context, throughout this paper we abuse the notation

$$C^r(\mathbb{R}^s)$$

to denote *either* the vector space of r times continuously differentiable functions from \mathbb{R}^s to \mathbb{R} which are not necessarily bounded, *or* the Banach space of all r times continuously differentiable functions from \mathbb{R}^s to \mathbb{R} with bounded derivatives of order up to r , normed by

$$\|f\|_{C^r(\mathbb{R}^s)} := \max_{\mu \in \mathcal{A}_r} \|\partial^\mu f\|_\infty.$$

2. Honeycomb subdivision

As the name suggests, a *honeycomb* subdivision scheme operates on *hexagon tilings*. On the left panel of Fig. 2, the solid lines depict a hexagon tiling \mathcal{X}^0 , whereas the dotted lines depict a refined hexagon tiling \mathcal{X}^1 . In this case, a tile (which is a regular hexagon) in the finer tiling has a side length half of that of a tile in the coarser tiling. Apparently, one can apply the refinement procedure recursively to produce finer and finer hexagon tilings $\mathcal{X}^n, n = 2, 3, \dots$. We denote by H^j the set of *vertices* of the hexagons in \mathcal{X}^j . Notice that H^n are nested, in fact

$$H^0 \subset H^1 \subset H^2 \subset \dots \subset \bigcup_{n=0}^\infty H^n \stackrel{\text{dense}}{\subset} \mathbb{R}^2. \tag{2.1}$$

What we have just described is the so-called *topological part* of a honeycomb subdivision scheme. A honeycomb subdivision process begins with numerical values associated with the coarsest lattice H^0 , denoted by $v^0: H^0 \rightarrow \mathbb{R}$. A honeycomb subdivision scheme is specified by a certain set of local rules used recursively to produce data defined on the finer and finer lattices H^n , i.e. the subdivision scheme would produce data $v^n: H^n \rightarrow \mathbb{R}, n = 1, 2, 3, \dots$ in a sequential manner. Such a subdivision scheme is said to be convergent if, for any bounded sequence v^0 , there exists a (unique) continuous function $f: \mathbb{R}^2 \rightarrow \mathbb{R}$, such that

$$\lim_{n \rightarrow \infty} \sup_{p \in H^n} |f(p) - v^n(p)| = 0. \tag{2.2}$$

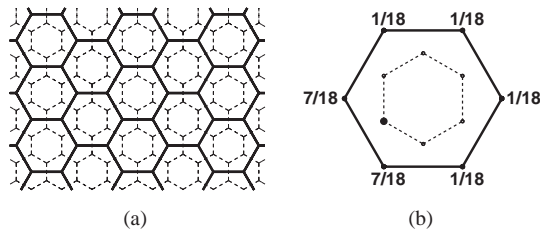


Fig. 3. (a) A Hexagon tiling and its “ $\sqrt{3}$ -refinement”; (b) A subdivision rule from [3].

For concreteness, we give an example of honeycomb subdivision scheme by Prautzsch [2], derived from the theory of box spline. In this subdivision scheme, $v^{n+1} : H^{n+1} \rightarrow \mathbb{R}$ is determined from $v^n : H^n \rightarrow \mathbb{R}$ as follows: for $p \in H^{n+1}$,

- if $p \in H^n$, and the 3 neighbors of p in \mathcal{X}^n are denoted by p_1, p_2 and p_3 , then
- if $p \notin H^n$, then p is inside a hexagon X in \mathcal{X}^n , we denote the vertices of X by $x_i, i = 0, \dots, 5$, and let x_0 be the vertex closest to p , and x_3 be the furthest one to p , then

$$v^{n+1}(p) := \frac{1}{2} \cdot v^n(x_0) + \frac{1}{8} \cdot [v^n(x_1) + v^n(x_2) + v^n(x_4) + v^n(x_5)].$$

See also Figs. 2(b) and (c).

The scheme we just described is by no means the only possible honeycomb subdivision scheme. One can for instance use subdivision rules with larger stencils to get smoother schemes. One can also change the topological part by choosing a refinement rule different from the one shown in Fig. 2(a). In Fig. 3(a), a different topological refinement rule is shown, unlike the one in Fig. 2(a), which increases the density of hexagons by a factor of 4, this rule increases the density by a factor of 3; and the vertex sets H^n of the successively refined tilings are not nested (cf. (2.1)), although it is still the case that $\bigcup_{n=0}^{\infty} H^n \stackrel{\text{dense}}{\subset} \mathbb{R}^2$. The simple subdivision rule depicted in Fig. 2(b) is claimed in [3] to be convergent in the sense of (2.2) with the limit function f being C^1 .

2.1. Connection to subdivision operator

In the wavelet literature, a bivariate subdivision scheme in the regular setting is usually defined by a linear operator $S := S_{\mathbf{a}, M} : [\ell(\mathbb{Z}^2)]^{1 \times m} \rightarrow [\ell(\mathbb{Z}^2)]^{1 \times m}$ of the form

$$Sv(\alpha) = \sum_{\beta \in \mathbb{Z}^2} v(\beta) \mathbf{a}(\alpha - M\beta), \tag{2.3}$$

where $\mathbf{a} \in [\ell^0(\mathbb{Z}^2)]^{m \times m}$ is the mask, M is the dilation matrix and m is the multiplicity of the subdivision operator. In this setting, a stationary subdivision scheme is one based on iteratively applying the operator S to a sequence of initial data $v^0 \in [\ell(\mathbb{Z}^2)]^{1 \times m}$ to obtain subdivision data

$$v^n := S^n v^0 \in [\ell(\mathbb{Z}^2)]^{1 \times m}.$$

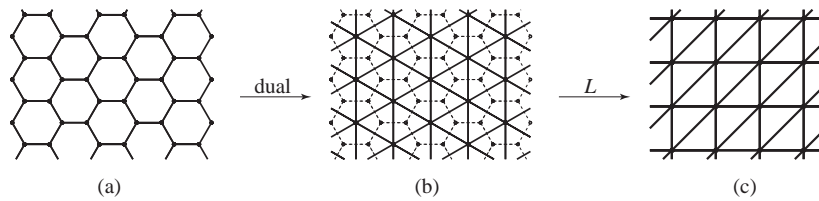


Fig. 4. (a) Tiling of \mathbb{R}^2 by regular hexagon with side length = 2^{-n} ; (b) the dual tiling of (a), which is a tiling by equilateral triangles with side length = $2^{-n}\sqrt{3}$; (c) a linear map L transforms the triangular tiling (b) into a triangular tiling made up of isosceles triangles, the set of vertices of these isosceles triangles is the point set $2^{-n}\mathbb{Z}^2$.

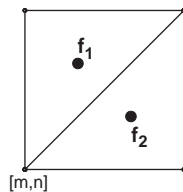


Fig. 5. As a convention, the two triangles with centroids f_1 and f_2 are associated with the lattice point $\alpha = [m, n]$. This, combined with Fig. 4, gives a 2–1 correspondence between H^n and $2^{-n}\mathbb{Z}^2$.

Such a subdivision scheme is said to be convergent if for any bounded initial data v^0 there exist (bounded) continuous functions f_1, \dots, f_m such that

$$\lim_{n \rightarrow \infty} \sup_{\alpha \in \mathbb{Z}^2} \|v^n(\alpha) - [f_1(M^{-n}\alpha), \dots, f_m(M^{-n}\alpha)]\|_\infty = 0.$$

While the definition in (2.3) seems quite general, at first glance it may seem rather unclear whether a honeycomb subdivision scheme described earlier can be cast as a specific case of (2.3): a honeycomb scheme operates on hexagonal lattices (2.1) whereas (2.3) operates on the lattices $M^{-n}\mathbb{Z}^2$. The catch is that there is a natural 2–1 correspondence between the hexagonal lattice H_j and the lattice $2^{-n}\mathbb{Z}^2$ for each $n = 0, 1, \dots$. See Fig. 4. This observation will allow us to rewrite a honeycomb subdivision scheme based on the refinement in Fig. 2(a) (resp. Fig. 3(a)) into the form (2.3) with

$$M = 2I_2 := \begin{bmatrix} 2 & 0 \\ 0 & 2 \end{bmatrix} \quad \text{and} \quad m = 2 \quad \left(\text{resp. } M = M_{\sqrt{3}} := \begin{bmatrix} 1 & -2 \\ 2 & -1 \end{bmatrix} \quad \text{and} \quad m = 2 \right).$$

Fig. 4 shows that there is a 1–1 correspondence of H^j with the set of centroids of the triangles in Fig. 4(c); the latter, in turn, can be put in a 2–1 correspondence with $2^{-n}\mathbb{Z}^2$, see Fig. 5. We note that the linear map responsible for transforming the tiling in Fig. 4(b) to the one in Fig. 4(c) is the following matrix independent of j :

$$L = \frac{1}{3} \begin{bmatrix} 2 & 0 \\ 1 & \sqrt{3} \end{bmatrix}. \tag{2.4}$$

With the above convention, and with the map $\alpha \mapsto 2^n \alpha$, we can identify the following three vector spaces:

$$\ell(H_n), \quad [\ell(2^{-n}\mathbb{Z}^2)]^{1 \times 2}, \quad [\ell(\mathbb{Z}^2)]^{1 \times 2}.$$

Then Prautzsch’s honeycomb subdivision scheme (Fig. 2) can be written in the form of (2.3) with multiplicity $m = 2$, dilation matrix $M = 2I_2$, and subdivision mask \mathbf{a} being

$$\begin{aligned} \mathbf{a}(-1, -1) &= \begin{bmatrix} c & 0 \\ 0 & c \end{bmatrix}, & \mathbf{a}(-1, 0) &= \begin{bmatrix} e & b \\ 0 & c \end{bmatrix}, & \mathbf{a}(-1, 1) &= \begin{bmatrix} b & c \\ 0 & 0 \end{bmatrix}, & \mathbf{a}(0, -1) &= \begin{bmatrix} c & 0 \\ b & e \end{bmatrix}, \\ \mathbf{a}(0, 0) &= \begin{bmatrix} a & b \\ b & a \end{bmatrix}, & \mathbf{a}(0, 1) &= \begin{bmatrix} a & d \\ 0 & e \end{bmatrix}, & \mathbf{a}(0, 2) &= \begin{bmatrix} c & b \\ 0 & 0 \end{bmatrix}, & \mathbf{a}(1, -1) &= \begin{bmatrix} 0 & 0 \\ b & c \end{bmatrix}, \\ \mathbf{a}(1, 0) &= \begin{bmatrix} e & 0 \\ d & a \end{bmatrix}, & \mathbf{a}(1, 1) &= \begin{bmatrix} a & b \\ b & a \end{bmatrix}, & \mathbf{a}(1, 2) &= \begin{bmatrix} e & b \\ 0 & c \end{bmatrix}, & \mathbf{a}(2, 0) &= \begin{bmatrix} 0 & 0 \\ b & c \end{bmatrix}, \\ \mathbf{a}(2, 1) &= \begin{bmatrix} c & 0 \\ b & e \end{bmatrix}, & \mathbf{a}(2, 2) &= \begin{bmatrix} c & 0 \\ 0 & c \end{bmatrix}, & \mathbf{a}(x) &= \mathbf{0} & \text{otherwise,} \end{aligned} \tag{2.5}$$

where $a = \frac{1}{2}, b = c = \frac{1}{8}, d = e = \frac{1}{4}$. Similarly, the honeycomb scheme shown in Fig. 3 can be written in the form of (2.3) with multiplicity $m = 2$, dilation matrix $M = M_{\sqrt{3}}$, and subdivision mask \mathbf{a} being

$$\begin{aligned} \mathbf{a}(-3, -2) &= \begin{bmatrix} c & c \\ 0 & 0 \end{bmatrix}, & \mathbf{a}(-3, -1) &= \begin{bmatrix} 0 & b \\ 0 & 0 \end{bmatrix}, & \mathbf{a}(-2, -2) &= \begin{bmatrix} b & 0 \\ 0 & 0 \end{bmatrix}, \\ \mathbf{a}(-2, -1) &= \begin{bmatrix} a & a \\ 0 & 0 \end{bmatrix}, & \mathbf{a}(-2, 0) &= \begin{bmatrix} b & a \\ c & b \end{bmatrix}, & \mathbf{a}(-2, 1) &= \begin{bmatrix} 0 & c \\ 0 & c \end{bmatrix}, \\ \mathbf{a}(-1, -1) &= \begin{bmatrix} a & b \\ b & c \end{bmatrix}, & \mathbf{a}(-1, 0) &= \begin{bmatrix} a & a \\ a & a \end{bmatrix}, & \mathbf{a}(-1, 1) &= \begin{bmatrix} c & b \\ b & a \end{bmatrix}, & \mathbf{a}(0, -1) &= \begin{bmatrix} c & 0 \\ c & 0 \end{bmatrix}, \\ \mathbf{a}(0, 0) &= \begin{bmatrix} b & c \\ a & b \end{bmatrix}, & \mathbf{a}(0, 1) &= \begin{bmatrix} 0 & 0 \\ a & a \end{bmatrix}, & \mathbf{a}(0, 2) &= \begin{bmatrix} 0 & 0 \\ 0 & b \end{bmatrix}, \\ \mathbf{a}(1, 1) &= \begin{bmatrix} 0 & 0 \\ b & 0 \end{bmatrix}, & \mathbf{a}(1, 2) &= \begin{bmatrix} 0 & 0 \\ c & c \end{bmatrix}, & \mathbf{a}(x) &= \mathbf{0} & \text{otherwise,} \end{aligned} \tag{2.6}$$

where $a = \frac{7}{18}, b = \frac{1}{18}, c = \frac{1}{18}$.

3. Two-fold and k -fold Hermite subdivision

For any vector sequence $v \in [\ell(\mathbb{Z}^2)]^{1 \times 2\#A_r}$,

$$v^1, v^2 \in [\ell(\mathbb{Z}^2)]^{1 \times \#A_r}$$

are defined such that $[v^1(\alpha), v^2(\alpha)] = v(\alpha), \alpha \in \mathbb{Z}^2$. Also, denote by $[\partial^{\leq r} f]|_{M^{-n}\mathbb{Z}^s}$ the element in $[\ell(\mathbb{Z}^s)]^{1 \times \#A_r}$ defined by $([\partial^{\leq r} f]|_{M^{-n}\mathbb{Z}^s})(\alpha) = (\partial^{\leq r} f)(M^{-n}\alpha)$.

Definition 3.1. A two-fold order r Hermite subdivision operator $S := S_{\mathbf{a}, M}$ is a subdivision operator (2.3) with multiplicity $m = 2\#A_r$ such that (i) for any initial sequence $v \in [\ell^0(\mathbb{Z}^2)]^{1 \times m}$, there exists

$f_v \in C^r(\mathbb{R}^2)$ such that

$$\lim_{n \rightarrow \infty} \|[\partial^{\leq r} f_v]_{M^{-n}\mathbb{Z}^2} - v_n^1 \mathcal{S}(M^n, A_r)\|_{[\ell^\infty(\mathbb{Z}^2)]^{1 \times \#A_r}} = 0, \tag{3.1}$$

$$\lim_{n \rightarrow \infty} \|[\partial^{\leq r} f_v]_{M^{-n}\mathbb{Z}^2} - v_n^2 \mathcal{S}(M^n, A_r)\|_{[\ell^\infty(\mathbb{Z}^2)]^{1 \times \#A_r}} = 0, \tag{3.2}$$

where $v_n = S^n v$, (ii) $f_v \neq 0$ for some $v \neq 0$.

For notational convenience, we write

$$S^\infty v := f_v.$$

Remark. A notion of k -fold order r Hermite subdivision operator in a general dimension s can be analogously defined. Such a definition will generalize our Definition 3.1 and also [10, Definition 1.1]. Theorem 3.3 below also has an obvious generalization to general k and s .

Caveat. Definition 3.1, although motivated by the study of honeycomb Hermite subdivision schemes, has applications in other contexts. For example, one can construct a new kind of subdivision scheme for, say, square tiling with refinement rule shown in Fig. 1(a) or (b), and with Hermite data attached to both the vertices and the centers of faces, such a subdivision scheme can then be precisely described as a two-fold Hermite subdivision operator; however, its dilation matrix and symmetry property will be entirely different from those of honeycomb Hermite subdivision schemes as described in Section 4. See also the remarks in Section 6.

3.1. Sum rules

(We work exclusively in dimension $s = 2$, although all the comments and results require only notation modification to carry over to the s -dimensional setting.)

The limit function f_v in Definition 3.1, when exists, is unique; in fact

$$f_v = \sum_{\alpha} v(\alpha) \phi(\cdot - \alpha),$$

where $\phi = (\phi_i)_{i=1}^m$ (as a column vector) is the “impulse response” of the subdivision scheme: $\phi_i := S^\infty(\delta e_i)$; here e_i is the i th coordinate unit vector in $\mathbb{R}^{1 \times m}$. The vector ϕ satisfies the well-studied two-scale refinement equation:

$$\phi(x) = \sum_{\alpha \in \mathbb{Z}^2} \mathbf{a}(\alpha) \phi(Mx - \alpha). \tag{3.3}$$

It is well-known from the theory of refinement equation that if Eq. (3.3) has a smooth solution $\phi \in [C^r(\mathbb{R}^s)]^m$ then the shift invariant space generated by ϕ has accuracy order $r + 1$, i.e.

$$\text{span}\{\phi(\cdot - \alpha) : \alpha \in \mathbb{Z}^2\} \supseteq \Pi_r \tag{3.4}$$

and if in addition $\text{span}\{\hat{\phi}(2\pi(M^T)^{-1}\alpha + 2\pi\beta) : \beta \in \mathbb{Z}^2\} = \mathbb{C}^m$ for all $\alpha \in \mathbb{Z}^2$, then the mask \mathbf{a} must satisfy the sum rules of order $r + 1$ (see [4, Theorem 2.4] and [5]): $\exists y \in [\ell^0(\mathbb{Z}^2)]^{1 \times m}$ such that $\hat{y}(0) \neq 0$,

$$D^\mu[\hat{y}(M^T \cdot) \hat{\mathbf{a}}(\cdot)](0) = D^\mu \hat{y}(0) \quad \forall |\mu| \leq r \tag{3.5}$$

and

$$D^\mu[\hat{y}(M^T \cdot) \hat{\mathbf{a}}(\cdot)](2\pi\beta) = 0 \quad \forall |\mu| \leq r, \quad \beta \in (M^T)^{-1} \mathbb{Z}^2 \setminus \mathbb{Z}^2. \tag{3.6}$$

Conversely, if \mathbf{a} satisfies the sum rules of order $r + 1$, then (3.4) must be true ([4, Theorem 2.4]). As we will see the Hermite property of a subdivision mask \mathbf{a} is related to the structure of the vector y above; from this the vector y is partially known and the mask \mathbf{a} can be determined from (3.5)–(3.6) up to certain degrees of freedom.

Given a mask $\mathbf{a} \in [\ell^0(\mathbb{Z}^2)]^{m \times m}$, recall that the associated cascade operator $Q := Q_{\mathbf{a}, M}$ is defined by

$$Qf = \sum_{\alpha \in \mathbb{Z}^2} \mathbf{a}(\alpha) f(M \cdot - \alpha). \tag{3.7}$$

Let f be a length m column vector of tempered distributions. We say that f satisfies the *moment conditions* of order $r + 1$ with respect to $y \in [\ell^0(\mathbb{Z}^2)]^{1 \times m}$ (see [5]) if

$$\hat{y}(0) \hat{f}(0) = 1 \quad \text{and} \quad D^\mu[\hat{y}(\cdot) \hat{f}(\cdot)](2\pi\beta) = 0, \quad \mu \in A_r, \quad \beta \in \mathbb{Z}^2 \setminus \{0\}. \tag{3.8}$$

Assume that (3.5) is satisfied with some vector y . We say that the cascade algorithm associated with mask \mathbf{a} and dilation matrix M converges in $C^r(\mathbb{R}^2)$ if for any compactly supported function vector $f \in [C^r(\mathbb{R}^2)]^m$ satisfying the moment conditions of order $r + 1$ with respect to y , the sequence $(Q_{\mathbf{a}, M}^n f)_{n=0}^\infty$ is a Cauchy sequence in $[C^r(\mathbb{R}^2)]^m$; consequently, there exists $\phi \in [C^r(\mathbb{R}^2)]^m$ such that

$$\lim_{n \rightarrow \infty} \|Q_{\mathbf{a}, M}^n f - \phi\|_{[C^r(\mathbb{R}^2)]^m} = 0.$$

In this case the limit ϕ is a solution of the refinement equation (3.3) and moreover, (3.5)–(3.6) are satisfied (see [5]).

It is well-known that (3.4) is equivalent to the existence of a $y \in [\ell^0(\mathbb{Z}^2)]^{1 \times m}$ such that (3.8) holds with f being replaced by ϕ . This vector y , in vague terms, determines *how* the function vector ϕ reproduces Π_r : in fact (3.8) is equivalent to saying that the so-called super-function $g := y * f := \sum_{\alpha} y(\alpha) f(\cdot - \alpha)$ satisfies $\sum_{\alpha} p(\alpha) g(\cdot - \alpha) \in \Pi_r$ for all $p \in \Pi_r$; alternatively,

$$p * (y * f) = (p * y) * f = \sum_{\beta \in \mathbb{Z}^2} [p(\beta - iD) \hat{y}](0) f(\cdot - \beta) \in \Pi_r \quad \forall p \in \Pi_r. \tag{3.9}$$

(Here $D = [D_1, \dots, D_s]$ is a vector of differential operators, and for a polynomial $p \in \Pi_r$, $p(\beta - iD)$ denotes the differential operator $\sum_{v \geq 0} (D^v p)(\beta) / v! (-iD)^v$.) In addition to (3.8), if $D^\mu[\hat{y}(\cdot) \hat{f}(\cdot)](0) = 0$ for all $\mu \in A_r \setminus \{0\}$, then $p = p * (y * f)$ for all $p \in \Pi_r$.

Being an iterative algorithm, a spectral quantity

$$v_\infty(\mathbf{a}, M)$$

determines whether the cascade algorithm with mask \mathbf{a} and dilation matrix M converges in C^k . For definition of $v_p(\mathbf{a}, M)$, $p \in [1, \infty]$, see [5, Section 4]. The quantity $v_p(\mathbf{a}, M)$ plays a fundamental role in the study of the convergence of vector cascade algorithms and smoothness of refinable function vectors [5]. For example, the cascade algorithm associated with mask \mathbf{a} and dilation matrix M converges in the

Sobolev space $W_p^k(\mathbb{R}^2)$ ($1 \leq p \leq \infty$) if and only if $v_p(\mathbf{a}, M) > k$. Let ϕ be the refinable function vector with the mask \mathbf{a} and the dilation matrix M . Then one always has

$$\sup\{v : \phi \in [W_p^k(\mathbb{R}^2)]^{m \times 1}\} =: v_p(\phi) \geq v_p(\mathbf{a}, M).$$

If in addition the shifts of ϕ are stable, then one has

$$v_p(\phi) = v_p(\mathbf{a}, M).$$

For detailed discussion on these issues, see [5]. When a cascade algorithm converges in $C^r(\mathbb{R}^2)$, the same vector y above essentially determines which are the initial function vectors f for which the cascade sequence $(Q^n f)_{n=1}^\infty$ converges:

Theorem 3.2 (Han [5, Theorem 4.3]). *Let $\mathbf{a} \in [\ell^0(\mathbb{Z}^2)]^{m \times m}$, M be an $s \times s$ isotropic dilation matrix, $y \in [\ell^0(\mathbb{Z}^2)]^{1 \times m}$ such that $\hat{y}(0) \neq 0$ and (3.5) holds for a non-negative integer k . Then the following are equivalent:*

- (i) *For every compactly supported function vector $f \in [C^k(\mathbb{R}^2)]^{m \times 1}$ such that f satisfies the moment conditions of order $k + 1$ with respect to y , $(Q_{\mathbf{a}, M}^n f)_{n=1}^\infty$ is a Cauchy sequence in $[C^k(\mathbb{R}^2)]^{m \times 1}$;*
- (ii) $v_\infty(\mathbf{a}, M) > k$.

This theorem happens to give a set of simple sufficient conditions for constructing two-fold Hermite type subdivision masks. We now present the main result of this section.

Theorem 3.3. *Let \mathbf{a} be a mask with multiplicity $m = 2\#A_r$. Suppose that $v_\infty(\mathbf{a}, M) > r$. Then $S_{\mathbf{a}, M}$ is a two-fold order r Hermite subdivision operator if \mathbf{a} satisfies the sum rules of order $r + 1$ with a sequence $y \in [\ell^0(\mathbb{Z}^2)]^{1 \times m}$ that satisfies the following property: there exist $c, c' \in \mathbb{R}^2$, $c \neq c'$, such that*

$$\frac{(-c - iD)^\mu}{\mu!} \hat{y}^1(0) = e_\mu^T, \quad \frac{(-c' - iD)^\mu}{\mu!} \hat{y}^2(0) = e_\mu^T, \quad \mu \in A_r. \quad (3.10)$$

Proof. See Appendix A.

3.2. Estimating $v_\infty(\mathbf{a}, M)$

The important spectral quantity $v_\infty(\mathbf{a}, M)$ is, in general, difficult to compute exactly, as it is equal to the joint spectral radius of two implicitly given matrices. However, if the mask \mathbf{a} satisfies sum rules of order $k + 1$ and also that 1 is a simple and dominant eigenvalue of the matrix

$$J_0 := \sum_{\beta \in \mathbb{Z}^2} \mathbf{a}(\beta) / |\det M|$$

and the first entry of its nonzero eigenvector for the eigenvalue 1 is nonzero, then one can lower bound $v_\infty(\mathbf{a}, M)$ by

$$v_\infty(\mathbf{a}, M) \geq -\log_{\rho(M)} \sqrt{\rho_k} - 1, \quad (3.11)$$

where ρ_k can be computed by the following procedure [11]: Let $b(\alpha) := \sum_{\beta} \overline{\mathbf{a}(\beta)} \otimes \mathbf{a}(\alpha + \beta) / |\det(M)|$ and

$$K := \mathbb{Z}^s \cap \sum_{n=1}^{\infty} M^{-n}(\text{supp } b). \tag{3.12}$$

Define the $m^2|K| \times m^2|K|$ matrix $F := (b(M\alpha - \beta))_{\alpha, \beta \in K}$. Denote the eigenvalues of M by $\sigma = (\sigma_1, \dots, \sigma_s)$. Let $J := \sum_{\alpha} a(\alpha) / |\det M|$, and $E_k = \{\lambda \overline{\sigma}^{-\mu}, \overline{\lambda} \sigma^{-\mu} : |\mu| \leq k, \lambda \in \text{spec}(J) \setminus \{1\}\} \cup \{\sigma^{-\mu} : |\mu| \leq 2k + 1\}$. Then

$$\rho_k := \max\{|\nu| : \nu \in \text{spec}(F) \setminus E_k\}.$$

In fact, $v_{\infty}(\mathbf{a}, M)$ is always a lower bound for the critical Hölder regularity of the refinable functions ϕ associated with mask (\mathbf{a}) and dilation matrix M and is exactly the critical Hölder regularity when the shifts of ϕ are stable. When the underlying ϕ has stable shifts and $k + 1$ is the highest sum rule order satisfied by \mathbf{a} , then $v_{\infty}(\phi) = v_{\infty}(\mathbf{a}, M)$ and $-\log_{\mathcal{E}_{\rho(M)}} \sqrt{\rho_k} = v_2(\mathbf{a}, M) = v_2(\phi)$, and (3.11) is a standard Sobolev embedding theorem in action.

4. Symmetric honeycomb Hermite subdivision

Throughout this section, we write

$$\mathbf{c}^1 = \left[\frac{1}{3}, \frac{2}{3}\right]^T, \quad \mathbf{c}^2 = \left[\frac{2}{3}, \frac{1}{3}\right]^T, \quad m = 2\#A_r. \tag{4.1}$$

A honeycomb Hermite subdivision scheme behaves in such a way that

$$S^n v(\alpha) \approx [D_n^{\leq r} f_v(M^{-n}(\alpha + \mathbf{c}^1), D_n^{\leq r} f_v(M^{-n}(\alpha + \mathbf{c}^2))] =: H_M^n(f_v), \quad n \text{ large}. \tag{4.2}$$

(Recall the notation defined in (1.3).)

The group of linear transforms that leaves a hexagon tiling (Fig. 4(a)) invariant is of course the dihedral group of the regular hexagon, denoted here by \mathcal{D}_6 ; we recall that the dihedral group of the regular k -gon is

$$\mathcal{D}_k := \{O_k^i, FO_k^i : i = 0, \dots, k - 1\}, \text{ where}$$

$$O_k := \begin{bmatrix} \cos(\frac{2\pi}{k}) & \sin(\frac{2\pi}{k}) \\ -\sin(\frac{2\pi}{k}) & \cos(\frac{2\pi}{k}) \end{bmatrix} \quad \text{and} \quad F := \begin{bmatrix} 1 & 0 \\ 0 & -1 \end{bmatrix}.$$

Since we are working with the 3-directional grid (Fig. 4(c)) instead of the hexagon tiling, we define

$$\begin{aligned} D_6 &:= \{LEL^{-1} : E \in \mathcal{D}_6\} \quad (L \text{ is the linear map (2.4)}) \\ &= \left\{ \pm \begin{bmatrix} 1 & 0 \\ 0 & 1 \end{bmatrix}, \pm \begin{bmatrix} 0 & -1 \\ 1 & -1 \end{bmatrix}, \pm \begin{bmatrix} -1 & 1 \\ -1 & 0 \end{bmatrix}, \pm \begin{bmatrix} 0 & 1 \\ 1 & 0 \end{bmatrix}, \pm \begin{bmatrix} 1 & -1 \\ 0 & -1 \end{bmatrix}, \pm \begin{bmatrix} -1 & 0 \\ -1 & 1 \end{bmatrix} \right\}. \end{aligned} \tag{4.3}$$

We shall need the following subgroup of D_6 :

$$D_6^1 = \{LO_6^{2i}L^{-1}, LFO_6^{2i+1}L^{-1} : i = 0, 1, 2\}.$$

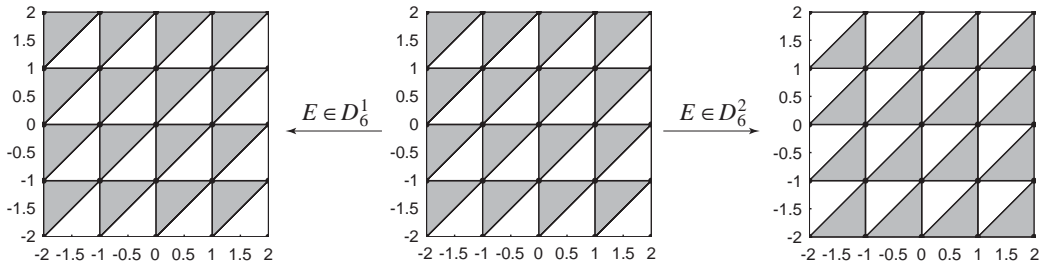


Fig. 6. Type I and type II triangles are the gray and the white triangles in the middle panel, respectively. Type I triangles contain the points $\mathbb{Z}^2 + \mathbf{c}^1$, Type II ones contain $\mathbb{Z}^2 + \mathbf{c}^2$.

We write also $D_6^2 = D_6 \setminus D_6^1$. If we define type I and type II triangles according to Fig. 6, then each element in D_6^1 , when acting on \mathbb{R}^2 , preserves the type of each triangle, whereas, an element in D_6^2 flips the type of each triangle.

Let G be a subgroup of D_6 . (In most of the rest of this article, G is simply D_6 .) We say that an isotropic dilation matrix M is compatible with G if

$$MEM^{-1} \in G, \quad \forall E \in G. \tag{4.4}$$

This condition is equivalent to saying that, for any (positive or negative) integer n ,

$$\{M^n EM^{-n} : E \in G\} = G. \tag{4.5}$$

In words, this condition means that the same matrix group G is used to describe symmetry on *any* dilated grid $M^{-n}\mathbb{Z}^2$, which happens to be a natural condition for studying symmetry properties of *stationary* subdivision schemes on hexagon tiling.

If M is compatible with G , then so is PMQ for any $P, Q \in G$; we say that two dilation matrices are G -equivalent if they are related this way. It is shown in [6] that any dilation matrix M compatible with D_6 must be D_6 -equivalent to either $M = dI_2$, $d \in \{2, 3, \dots\}$, or $M = dM_{\sqrt{3}}$, $d \in \{1, 2, 3, \dots\}$. The following “ $\sqrt{7}$ dilation matrix”:

$$M = \begin{bmatrix} 3 & -1 \\ 1 & 2 \end{bmatrix}$$

is not compatible with D_6 but with the subgroup

$$R_6 := \{LO_6^i L^{-1} : i = 0, \dots, k - 1\}.$$

We define a Hermite data sampler $H_M^n : C^r(\mathbb{R}^2) \rightarrow [\ell(\mathbb{Z}^2)]^{1 \times m}$ by

$$H_M^n(f)(\alpha) := [D_n^{\leq r} f(M^{-n}(\alpha + \mathbf{c}^1)), D_n^{\leq r} f(M^{-n}(\alpha + \mathbf{c}^2))]. \tag{4.6}$$

Notice how this definition is tied to the convention depicted in Fig. 5.

Definition 4.1. Let G be a subgroup of D_6 and M be a dilation matrix compatible with G . We say that a two-fold order r Hermite subdivision operator $S = S_{\mathbf{a},M}$ is a G -symmetric honeycomb Hermite subdivision operator if for any $f \in C^r(\mathbb{R}^2)$ and $E \in G$, if $v := H_M^0(f)$ and $w := H_M^0(g)$, where $g := f(E\cdot)$, then $S^\infty w = (S^\infty v)(E\cdot)$.

Note that for a function $f \in C^r(\mathbb{R}^2)$, and $g := f(E\cdot)$, $E \in D_6$, there is a unique linear operator $T_E^n : [\ell(\mathbb{Z}^2)]^{1 \times m} \rightarrow [\ell(\mathbb{Z}^2)]^{1 \times m}$, such that $H_M^n(g) = T_E^n(H_M^n(f))$; this operator has the following explicit description: if $v \in [\ell(\mathbb{Z}^2)]^{1 \times m}$ and $w = T_E^n v$, then

$$\begin{aligned} \text{if } M^n E M^{-n} \in D_6^1, & w^1(\alpha) = v^1(\lfloor M^n E M^{-n}(\alpha + \mathbf{c}^1) \rfloor) \mathcal{S}(M^n E M^{-n}, A_r), \\ & w^2(\alpha) = v^2(\lfloor M^n E M^{-n}(\alpha + \mathbf{c}^2) \rfloor) \mathcal{S}(M^n E M^{-n}, A_r); \\ \text{if } M^n E M^{-n} \in D_6^2, & w^1(\alpha) = v^2(\lfloor M^n E M^{-n}(\alpha + \mathbf{c}^2) \rfloor) \mathcal{S}(M^n E M^{-n}, A_r), \\ & w^2(\alpha) = v^1(\lfloor M^n E M^{-n}(\alpha + \mathbf{c}^1) \rfloor) \mathcal{S}(M^n E M^{-n}, A_r). \end{aligned} \tag{4.7}$$

In above and below, we write

$$\lfloor v \rfloor := [\lfloor v(1) \rfloor, \lfloor v(2) \rfloor]^T$$

for $v \in \mathbb{R}^2$. Note, however, that in all applications of this notation the operand v is either in $\mathbb{Z}^2 + \mathbf{c}^1$ or $\mathbb{Z}^2 + \mathbf{c}^2$; thus our usage of this notation is actually parallel to the convention depicted in Fig. 5.

For a two-fold Hermite subdivision mask \mathbf{a} , we decompose each matrix $\mathbf{a}(\alpha) \in \mathbb{R}^{2\#A_r \times 2\#A_r}$, $\alpha \in \mathbb{Z}^2$ into four $\#A_r \times \#A_r$ sub-matrices $\mathbf{a}^{1,1}(\alpha)$, $\mathbf{a}^{1,2}(\alpha)$, $\mathbf{a}^{2,1}(\alpha)$ and $\mathbf{a}^{2,2}(\alpha)$ in the following manner:

$$\mathbf{a}(\alpha) = \begin{bmatrix} \mathbf{a}^{1,1}(\alpha) & \mathbf{a}^{1,2}(\alpha) \\ \mathbf{a}^{2,1}(\alpha) & \mathbf{a}^{2,2}(\alpha) \end{bmatrix}.$$

Theorem 4.2. A two-fold order r Hermite subdivision operator $S = S_{\mathbf{a},M}$ is a G -symmetric honeycomb Hermite subdivision operator if any one of the following equivalent conditions is satisfied:

- (i) $S_{\mathbf{a},M} \circ T_E^n = T_E^{n+1} \circ S_{\mathbf{a},M}$, $\forall E \in G$, $n = 0, 1, 2, \dots$
- (ii) $S_{\mathbf{a},M} \circ T_E^0 = T_E^1 \circ S_{\mathbf{a},M}$, $\forall E \in G$.
- (iii) $(S_{\mathbf{a},M} \circ T_E^0)(\delta e_i^T) = T_E^1 \circ S_{\mathbf{a},M}(\delta e_i^T)$, $\forall E \in G$, $i = 1, \dots, m$, where $\{e_i, i = 1, \dots, m\}$ is the standard basis of \mathbb{R}^m . (The notation δe_i^T refers to the element $v \in [\ell(\mathbb{Z}^2)]^{1 \times m}$ with $v(\alpha)$ equals to e_i^T when $\alpha = [0, 0]^T$ and the zero vector otherwise.)

Proof. See Appendix B.

It is clear that condition (iii) in Theorem 4.2 is equivalent to a finite set of linear conditions on the (finitely supported) mask \mathbf{a} . Based on (4.7) and a routine derivation, these linear conditions can be written down explicitly as follows: $\forall \beta \in \mathbb{Z}^2$, $E \in G$, if

$$\begin{aligned} \alpha_1 &= \lfloor M E M^{-1}(\beta + \mathbf{c}^1) \rfloor, & \alpha_3 &= \beta - M \lfloor E^{-1} \mathbf{c}^1 \rfloor, \\ \alpha_2 &= \lfloor M E M^{-1}(\beta + \mathbf{c}^2) \rfloor, & \alpha_4 &= \beta - M \lfloor E^{-1} \mathbf{c}^2 \rfloor, \end{aligned}$$

then

$$\mathcal{S}_{E^{-1}} \begin{bmatrix} \mathbf{a}^{1,1}(\alpha_1), \mathbf{a}^{1,2}(\alpha_2) \\ \mathbf{a}^{2,1}(\alpha_1), \mathbf{a}^{2,2}(\alpha_2) \end{bmatrix} \mathcal{S}_{MEM^{-1}} = \begin{bmatrix} \mathbf{a}^{1,1}(\alpha_3), \mathbf{a}^{1,2}(\alpha_3) \\ \mathbf{a}^{2,1}(\alpha_4), \mathbf{a}^{2,2}(\alpha_4) \end{bmatrix}$$

if $E \in D_6^1$ and $MEM^{-1} \in D_6^1$; (4.8)

$$\mathcal{S}_{E^{-1}} \begin{bmatrix} \mathbf{a}^{1,1}(\alpha_1), \mathbf{a}^{1,2}(\alpha_2) \\ \mathbf{a}^{2,1}(\alpha_1), \mathbf{a}^{2,2}(\alpha_2) \end{bmatrix} \mathcal{S}_{MEM^{-1}} = \begin{bmatrix} \mathbf{a}^{2,1}(\alpha_3), \mathbf{a}^{2,2}(\alpha_3) \\ \mathbf{a}^{1,1}(\alpha_4), \mathbf{a}^{1,2}(\alpha_4) \end{bmatrix}$$

if $E \in D_6^2$ and $MEM^{-1} \in D_6^1$; (4.9)

$$\mathcal{S}_{E^{-1}} \begin{bmatrix} \mathbf{a}^{1,2}(\alpha_1), \mathbf{a}^{1,1}(\alpha_2) \\ \mathbf{a}^{2,2}(\alpha_1), \mathbf{a}^{2,1}(\alpha_2) \end{bmatrix} \mathcal{S}_{MEM^{-1}} = \begin{bmatrix} \mathbf{a}^{1,1}(\alpha_3), \mathbf{a}^{1,2}(\alpha_3) \\ \mathbf{a}^{2,1}(\alpha_4), \mathbf{a}^{2,2}(\alpha_4) \end{bmatrix}$$

if $E \in D_6^1$ and $MEM^{-1} \in D_6^2$; (4.10)

$$\mathcal{S}_{E^{-1}} \begin{bmatrix} \mathbf{a}^{1,2}(\alpha_1), \mathbf{a}^{1,1}(\alpha_2) \\ \mathbf{a}^{2,2}(\alpha_1), \mathbf{a}^{2,1}(\alpha_2) \end{bmatrix} \mathcal{S}_{MEM^{-1}} = \begin{bmatrix} \mathbf{a}^{2,1}(\alpha_3), \mathbf{a}^{2,2}(\alpha_3) \\ \mathbf{a}^{1,1}(\alpha_4), \mathbf{a}^{1,2}(\alpha_4) \end{bmatrix}$$

if $E \in D_6^2$ and $MEM^{-1} \in D_6^2$; (4.11)

where $\mathcal{S}_E := \mathcal{S}(E, A_r) \oplus \mathcal{S}(E, A_r)$ for any matrix E .

Remark. Although results on symmetry similar to Theorem 4.2 can be found in [8,10], the method of proof here (see Appendix B) seems more intuitive and, perhaps more significantly, does *not* require the technical condition that 1 is a simple and dominant eigenvalue of the matrix $J_0 := \sum_{\beta \in \mathbb{Z}^2} \mathbf{a}(\beta) / |\det M|$ and the first entry of its nonzero eigenvector for the eigenvalue 1 is nonzero. (The corresponding symmetry results in [8,10] require the latter technical condition.)

5. Examples

In surface design, one typically desire surfaces which are at least C^1 and preferably C^2 . C^2 , in a “practical sense”, actually means that the 2nd derivatives have to be sufficiently regular, preferably close to be Lipschitz; in mathematical terms it means that the critical Hölder regularity has to be significantly higher than 2. We know that the $M = 2I_2$ mask in (2.5) comes from a C^1 spline, so has a critical Hölder regularity exactly equals to 2. (But the scheme is *not* C^2 .) The critical Hölder regularity of $\sqrt{3}$ scheme with the mask (2.6) is estimated to be 2.1239 [12, Table 6]. (Note: the lower bound (3.11) based on L^2 regularity only gives $v_\infty(a, M) \geq 2.6724 - 1$.) Furthermore, one can verify rigorously that, using techniques from subdivision theory, in fact any variant of the two honeycomb subdivision schemes in Section 2 with the same support cannot have a critical Hölder smoothness significantly higher than 2. See [12] for extensive computational results in this aspect.

In our terminology, the schemes in Section 2 are D_6 -symmetric honeycomb Hermite subdivisions schemes of order 0. Using Theorems 3.3 and 4.2, we construct in this section order 1 versions of these two schemes which are “ C^2 in a practical sense”.

For each of the cases of $M = 2I_2$ and $M = M_{\sqrt{3}}$, we consider D_6 -symmetry honeycomb Hermite subdivision mask of order 1 with the same support as in (2.5) and (2.6), respectively. We omit some of the computational tricks, which are documented in details in [8,10]; instead we focus on reporting the computational findings.

Solving by MAPLE for the mask entries based on

- the *nonlinear* constraints of sum rules (3.5)–(3.6), (3.10) with $c = \mathbf{c}^1$, $c' = \mathbf{c}^2$ (see the comments in Section 6), and
- the *linear* symmetry constraints (4.8)–(4.11) for the full symmetry group $G = D_6$,

we obtain the following results:

- For $M = 2I_2$, $r = 1$ and support size same as that of (2.5), we found the following parametric mask \mathbf{a} with 13 free parameters that satisfies D_6 -symmetry and sum rules of order 4 w.r.t. a y that satisfies (3.10). (Caution: the latter means that \mathbf{a} satisfies (3.5)–(3.6) for $r = 3$ w.r.t. a y that satisfies (3.10) for $r = 1$. Beware of the potential confusion with the notation r here.)

$$\mathbf{a}^{1,1}(0, 0) = \begin{bmatrix} \frac{5}{8} + 6t_2 - 6t_{10} & 0 & 3t_4 - 6t_{12} + \frac{1}{16} + 3t_8 + 3t_1 - 6t_9 + 3t_{13} \\ -\frac{1}{16} + t_7 + t_5 & t_4 & t_1 \\ -\frac{1}{8} + 2t_7 + 2t_5 & 0 & 2t_1 + t_4 \end{bmatrix},$$

$$\mathbf{a}^{1,2}(0, 0) = \begin{bmatrix} \frac{1}{8} - 3t_7 - 6t_2 + 3t_{10} & -\frac{3}{8} - 2t_{13} + 3t_9 + 3t_{12} & -t_{13} + \frac{5}{4} + 3t_{12} - 6t_1 \\ & & -6t_4 + 3t_9 - 6t_8 \\ & -t_5 + t_{10} & t_{12} - \frac{1}{3}t_{13} - 2t_1 + t_9 \\ & & -t_4 - t_8 + \frac{1}{6} \\ & -t_5 & -\frac{1}{3}t_{13} - 2t_1 + t_9 - t_4 \\ & & -t_8 + \frac{1}{6} \end{bmatrix},$$

$$\mathbf{a}^{1,1}(2, 2) = \begin{bmatrix} \frac{1}{16} + 3t_7 + 3t_2 & 3t_{12} + \frac{9}{16} - 3t_1 + 3t_9 & -3t_{12} - \frac{9}{16} + t_{13} + 3t_1 \\ & -3t_4 - 3t_8 & -3t_9 + 3t_4 + 3t_8 \\ t_7 & \frac{1}{8} + t_6 - \frac{1}{3}t_{13} + 2t_9 & -\frac{1}{8} - t_6 + \frac{1}{3}t_{13} + t_4 \\ & -t_4 - t_1 + t_{12} - t_8 & +t_1 - t_{12} + t_8 - t_9 \\ t_2 + t_7 & \frac{3}{16} - t_4 - t_1 + t_{12} & -\frac{1}{8} + \frac{1}{3}t_{13} + t_4 + t_1 \\ & -t_8 + t_9 & -t_{12} + t_8 - t_9 \end{bmatrix},$$

$$\mathbf{a}^{1,2}(0, 1) = \begin{bmatrix} \frac{3}{8} & 0 & 0 \\ 0 & t_3 & 0 \\ 0 & 0 & t_3 \end{bmatrix},$$

$$\mathbf{a}^{2,2}(0, 1) = \begin{bmatrix} \frac{5}{24} & -3t_{11} - t_3 + \frac{1}{2} & 3t_{11} + t_3 - \frac{1}{2} \\ -\frac{1}{72} & t_{11} & -\frac{1}{3}t_3 + \frac{1}{24} \\ \frac{1}{72} & -\frac{1}{3}t_3 + \frac{1}{24} & t_{11} \end{bmatrix}.$$

- For $M = M_{\sqrt{3}}$, $r = 1$ and support size same as that of (2.6), there exists the following parametric mask \mathbf{a} with 15 free parameters that satisfies D_6 -symmetry and sum rules of order 4 with respect to a y that satisfies (3.10).

$$\mathbf{a}^{2,1}(0,0) = \begin{bmatrix} \frac{7}{18} - t_{10} - 3t_{11} & \frac{7}{6} - t_{13} - t_{15} & t_{13} \\ +3t_{14} - 3t_3 & +3t_5 + 3t_6 & \\ \frac{1}{3}t_{10} + t_3 + t_{11} & t_7 & -t_7 + t_{12} \\ +\frac{1}{6}t_1 - \frac{1}{108} & & \\ t_{14} & -2t_{12} - \frac{1}{3}t_{13} + \frac{1}{3}t_{15} & 2t_5 + 2t_{12} + \frac{1}{3}t_{13} \\ & -3t_5 + t_7 - \frac{1}{9} - t_6 & -\frac{1}{3}t_{15} - t_7 + \frac{1}{9} + t_6 \end{bmatrix},$$

$$\mathbf{a}^{1,1}(0,0) = \begin{bmatrix} \frac{1}{9} + 3t_{11} & -\frac{5}{3} + t_{15} + t_{13} + 3t_5 & \frac{1}{3} - t_{13} - 3t_5 + 6t_9 \\ -3t_{14} + 3t_3 & -6t_9 - 3t_4 - 3t_2 + 3t_6 & +3t_4 + 3t_2 - 3t_6 \\ -\frac{1}{27} + \frac{1}{3}t_{10} & -t_6 + 2t_{12} + \frac{1}{3}t_{13} - \frac{1}{3}t_{15} + t_5 & -2t_{12} - \frac{1}{3}t_{13} + \frac{1}{3}t_{15} - t_5 \\ -t_{14} - \frac{1}{3}t_1 & -t_7 + 2t_9 + t_4 + t_2 - \frac{1}{18} & +t_7 - 2t_9 - t_4 - t_2 + \frac{1}{18} \\ -\frac{1}{18} - t_{11} & \frac{13}{9} + 2t_{12} - \frac{2}{3}t_{13} - \frac{4}{3}t_{15} - t_7 & -\frac{5}{9} - t_8 - 2t_{12} + \frac{1}{3}t_{13} \\ & +6t_9 + 4t_4 + 3t_2 - 2t_6 + \frac{1}{162t_1} & +\frac{2}{3}t_{15} + t_7 - 4t_9 \\ & & -2t_4 - 2t_2 + t_6 - \frac{1}{324t_1} \end{bmatrix},$$

$$\mathbf{a}^{1,1}(2,2) = \begin{bmatrix} t_{10} & -\frac{3}{2} + t_{15} - 6t_9 - 3t_4 & \frac{17}{6} - 2t_{15} + 6t_9 + 3t_4 \\ & -3t_2 + t_{13} - \frac{1}{108t_1} & +3t_2 - 2t_{13} + \frac{1}{54t_1} \\ -\frac{1}{3}t_{10} - t_3 - \frac{1}{6}t_1 + \frac{1}{108} & -t_4 + t_8 & t_4 \\ & t_8 + t_9 + t_2 & -t_2 \end{bmatrix}.$$

In each case above, the rest of the mask is given by the symmetry conditions (4.8)–(4.11). Notice that the 13-parameter mask for $M = 2I_2$ actually depends *linearly* on all the parameters, but the 15-parameter mask for $M = M\sqrt{3}$ depends linearly only on t_2, \dots, t_{15} , and *rationally* on t_1 .

Using Jia and Jiang's method as described in Section 3.2, together with the unconstrained minimization routine `fminu()` in the optimization toolbox of MATLAB, in each of the two cases above we attempt to minimize the lower bound (3.11) over the corresponding parameter space. The following results are obtained:

- For the 13 parameter mask above for $M = 2I_2$ and sum rules of order 4,

$$(t_i)_{i=1}^{13} = (0.0084, -0.0088, 0.1033, 0.0246, 0.0321, 0.0307, 0.0138, 0.0965, -0.0124, \dots, 0.0353, -0.0095, -0.0584, -0.2169) \quad (5.1)$$

gives $v_\infty(\mathbf{a}, M) \geq 3.3171 - 1$. We denote the first three and the last three components of the associated refinable function vector ϕ by ϕ_v^1 and ϕ_v^2 , $v \in A_1$, respectively. See Fig. 7 for the plots of these functions.

- For the 15 parameter mask above for $M = M\sqrt{3}$ and sum rules of order =4,

$$(t_i)_{i=1}^{15} = (-0.0117, 0.0952, 0.0222, -0.1532, -0.0029, -0.1459, 0.0129, \dots, -0.0215, -0.0002, -0.0063, -0.0353, 0.0416, 0.3292, 0.0001, 0.5727) \quad (5.2)$$

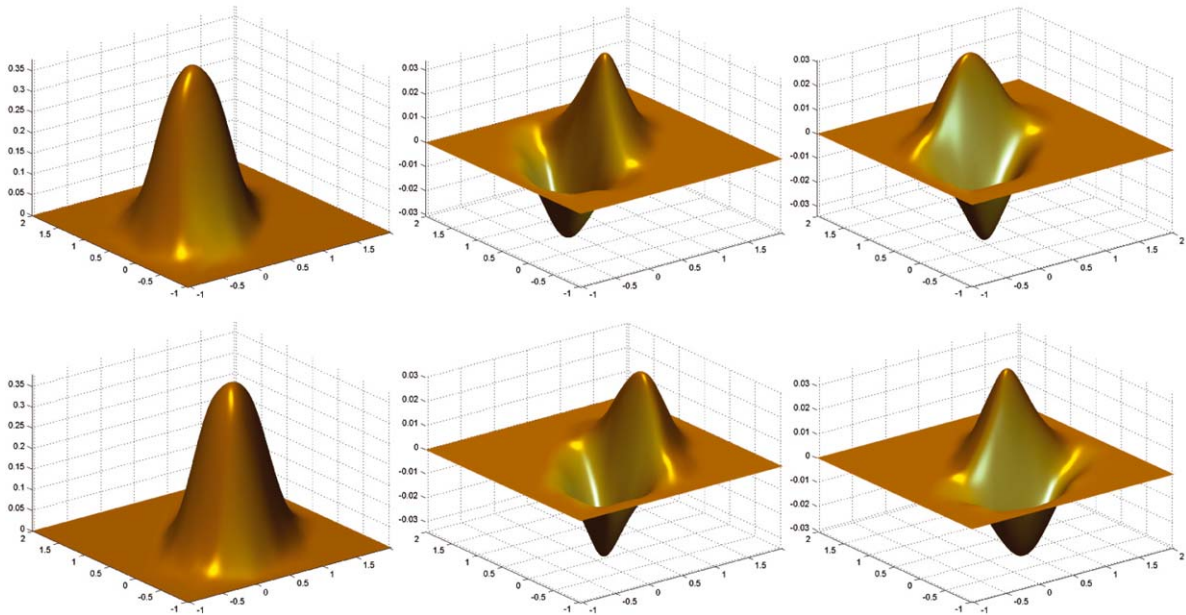


Fig. 7. From left to right, top to bottom: $\phi_{(0,0)}^1, \phi_{(1,0)}^1, \phi_{(0,1)}^1, \phi_{(0,0)}^2, \phi_{(1,0)}^2, \phi_{(0,1)}^2$. Note that the first three component functions are localized at the triangle bounded by $[0, 0]^T, [0, 1]^T, [1, 1]^T$, whereas the last three component functions are localized at the triangle bounded by $[0, 0]^T, [1, 0]^T, [1, 1]^T$.

gives $v_\infty(\mathbf{a}, M) \geq 3.2772 - 1$, whereas the parameters

$$(t_i)_{i=1}^{15} = (-0.0036, -0.0194, 0.0024, 0.0028, 0.0052, -0.0012, -0.0009, 0.0302, \dots, 0.0321, 0.1007, -0.0290, 0.0702, -0.3324, -0.0216, 0.1657) \tag{5.3}$$

gives $v_\infty(\mathbf{a}, M) \geq 3.4960 - 1$. See Fig. 8 for the plots of the associated refinable function vector corresponding to (5.2) and (5.3).

In both cases, the lower bound of $v_\infty(\mathbf{a}, M)$ exceeds 2, meaning that the corresponding refinable function vector consists of functions which are smoother than C^2 . We comment that the lower bound (3.11), coming from a Sobolev embedding theorem in dimension 2, is not tight, from our experience there is typically a significant gap (approximately 0.5 in a lot of cases) between the lower bound and the true $v_\infty(\mathbf{a}, M)$. So we can say in good confidence that the 2nd derivatives of the refinable functions associated with the schemes above are more than merely continuous.

Comments on fairness and smoothness: Fairness is a jargon in the CAGD literature; see, e.g., [13]. A fair surface is one that does not “exhibit unnecessary undulations”. The basis functions in Fig. 7 exhibit much less undulations when compared to those in Fig. 8. This is rather unexpected by the authors, as we never encountered a similar experience in our previous work: in either interpolatory [9] or non-interpolatory [10] vertex-based Hermite subdivision schemes we had constructed, the refinable functions for $M = 2I_2$ and $M = M_{\sqrt{3}}$ (with comparable support sizes) are equally fair, and all of them have a visual fairness significantly superior to that of those in Fig. 8.

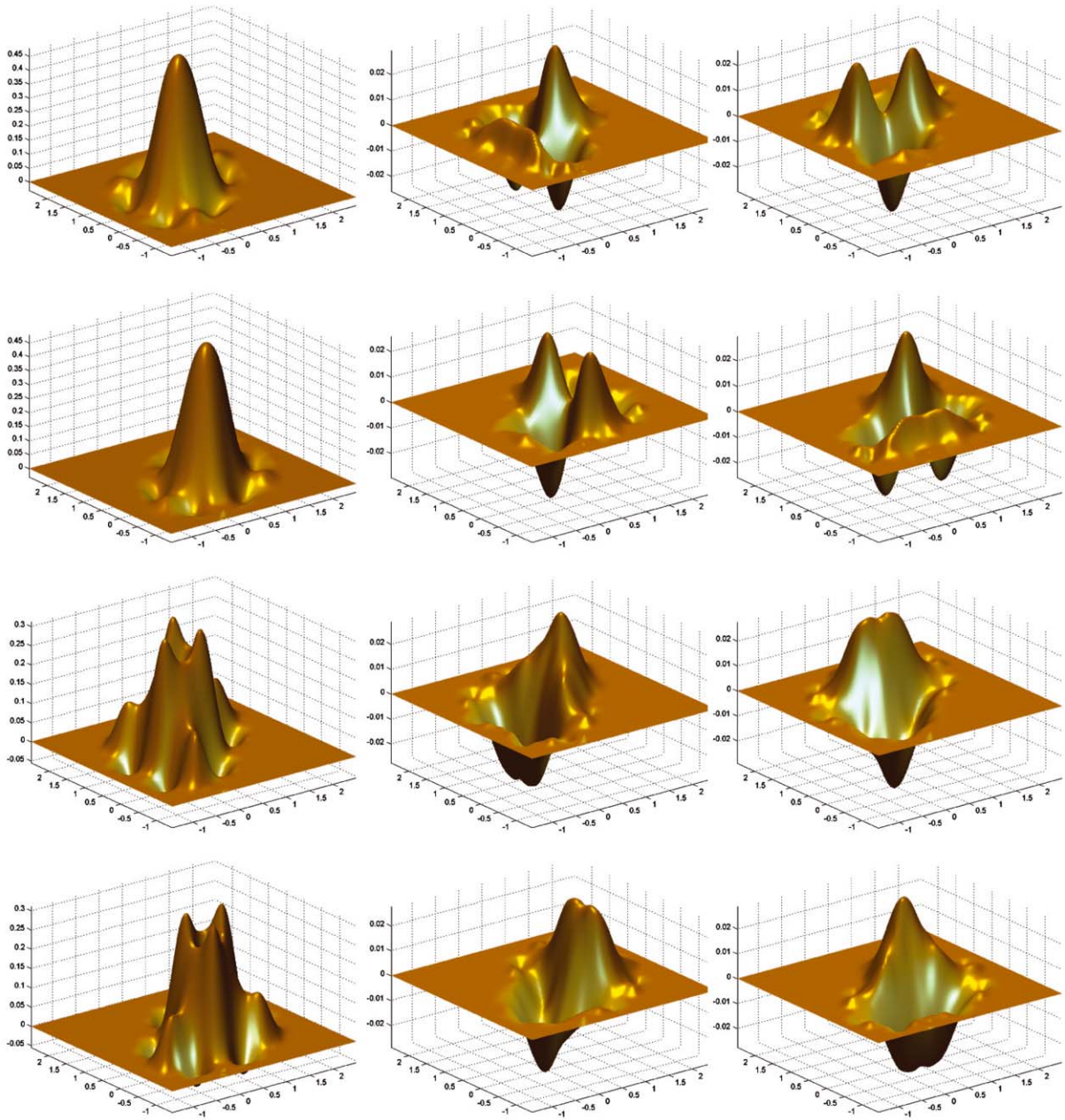


Fig. 8. The 6 component functions of ϕ for the 15-parameter mask in the case of $M = M\sqrt{3}$, with parameters listed in (5.2) and (5.3). The component functions are ordered similarly as in Fig. 7. Notice the lack of “fairness”, despite the comparable smoothness with that of the ϕ depicted in Fig. 7.

On the other hand, it is a very challenging computational problem to optimize smoothness and/or fairness over a parameter space of dimension 15. Recall that we optimize smoothness by maximizing

the lower bound on the right-hand side of (3.11), which is a *spectral radius minimization problem*. Such a problem is typically a non-smooth optimization problem, and a standard optimization method like the one we used is known to be inefficient and may yield very suboptimal results. While we settle with our “success” in finding C^2 schemes here, we plan to report elsewhere our results in attacking the computationally challenging optimization problems arisen from this article, based on using more appropriate non-smooth optimization tools (see [7] and the references therein). Furthermore, while we only optimize smoothness in our work, one may argue that optimizing smoothness and fairness are *conflicting* goals. We plan to explore these issues more carefully elsewhere.

6. Conclusion and remarks

In this paper we construct symmetric honeycomb Hermite subdivision schemes. Some of the subtleties in the theory deserve attention:

- Based on (4.2), one may be inclined to define a honeycomb subdivision operator as in Definition 3.1 but with (3.1)–(3.2) replaced by

$$\lim_{n \rightarrow \infty} \|[\partial^{\leq r} f_v]_{M^{-n}(\mathbb{Z}^2 + \mathbf{c}^i)} - v_n^i \mathcal{S}(M^n, A_r)\|_{[\ell^\infty(\mathbb{Z}^2)]^{1 \times \#A_r}} = 0, \quad i = 1, 2. \tag{6.1}$$

However, notice that at fine scales, i.e. when n is large, saying (4.2) is essentially the same as saying

$$S^n v(\alpha) \approx [D_n^{\leq r} f_v(M^{-n} \alpha), D_n^{\leq r} f_v(M^{-n} \alpha)]; \tag{6.2}$$

indeed an application of triangle inequality shows that (6.1) is *equivalent* to (3.1)–(3.2). This is why the concept of two-fold Hermite subdivision schemes (i.e. Definition 3.1) and the associated Theorem 3.3 are the right tools for the study of honeycomb Hermite subdivision schemes.

- Symmetry, on the other hand, is *not* an asymptotic issue, therefore symmetry properties of honeycomb Hermite subdivision schemes are very tied to (4.2). Recall Definition 4.1.
- In Section 5, we use Theorems 3.3 and 4.2 to construct symmetric honeycomb Hermite subdivision schemes. We notice that the sum rule conditions (3.10) in Theorems 3.3 involve two unknown vectors c and c' ; while in our computational framework in Section 5 we can always treat these two vectors as variables, we consistently see from our computation that any D_6 -symmetric honeycomb Hermite subdivision mask must satisfy a sum rule condition with a sequence y that satisfies (3.10) with

$$c = \mathbf{c}^1, \quad c' = \mathbf{c}^2. \tag{6.3}$$

Although in our theoretical development we treat sum rule and symmetry conditions independently, these conditions are somehow correlated. Intuitively it is because of the fact that sum rule conditions are primarily about polynomial reproduction, but at the same time polynomial spaces are symmetric in the sense that they are invariant under affine transformations.

A natural conjecture, then, is that the mask of a D_6 -symmetric honeycomb Hermite subdivision operator of order r must satisfy the sum rules of order $r + 1$ with a sequence $y \in [\ell^0(\mathbb{Z}^2)]^{1 \times m}$ that satisfies (3.10) and (6.3).

Acknowledgements

This work was supported by an NSF CAREER Award (CCR 9984501.) We thank Peter Oswald for helpful discussions.

Appendix A. Proof of Theorem 3.3

We need the following lemma, which generalizes [9, Lemma 2.6].

Lemma A.1. *Let c^1, \dots, c^k be distinct vectors in $[0, 1]^s$. For any $s \geq 1, r \geq 0, l > 0, r' \geq r$, there exists a*

$$\psi = \begin{bmatrix} \psi^1 \\ \vdots \\ \psi^k \end{bmatrix} \in [C^{r'}(\mathbb{R}^s)]^{k \times \#A_r}$$

(i.e. $\psi^i \in [C^{r'}(\mathbb{R}^s)]^{\#A_r}$) with accuracy order l and

$$\partial^{\leq r} \psi^i(\alpha + c^j) = \delta_{i,j} \delta_{\alpha,0} I_{\#A_r \times \#A_r}, \tag{A.1}$$

where for $[f_\mu]_{\mu \in A_r} \in [C^r(\mathbb{R}^s)]^{\#A_r}$, $\partial^{\leq r} f(x)$ is the $\#A_r \times \#A_r$ matrix with the μ th row equals to $\partial^{\leq r} f_\mu(x)$.

Proof. For a $v \in [\ell(\mathbb{Z}^s)]^{k \times \#A_r}$, let $v_j \in [\ell(\mathbb{Z}^s)]^{1 \times \#A_r}$ be defined by $v_j(\alpha)_\mu = v(\alpha)_{j,\mu}$. Constructing a ψ in the theorem is equivalent to constructing a local linear shift invariant operator

$$\mathcal{J} : [\ell(\mathbb{Z}^s)]^{k \times \#A_r} \rightarrow C^{r'}(\mathbb{R}^s)$$

such that

$$(\partial^{\leq r} \mathcal{J}(v))(\alpha + c^j) = v_j(\alpha), \quad j = 1, \dots, k, \quad \alpha \in \mathbb{Z}^s, \tag{A.2}$$

and

$$p \in \Pi_{l-1}, \quad v_j(\alpha) = \partial^{\leq r} p(\alpha + c^j) \implies \mathcal{J}(v) = p. \tag{A.3}$$

Eq. (A.2) means when Hermite data is prescribed on the lattice $\bigcup_{1 \leq j \leq k} (\mathbb{Z}^s + c^j)$, then \mathcal{J} can find a smooth function that interpolates the Hermite data. (A.3) means if Hermite data is sampled on the lattice $\bigcup_{1 \leq j \leq k} (\mathbb{Z}^s + c^j)$ from any polynomial of degree less than l , then \mathcal{J} can recover the polynomial exactly.

We use an old trick called ‘‘boolean sum’’ [1] to construct such an operator \mathcal{J} . We first construct two local linear shift-invariant operators I and $A : [\ell(\mathbb{Z}^s)]^{k \times \#A_r} \rightarrow C^{r'}(\mathbb{R}^s)$ such that

- I satisfies (A.2) but may not satisfy (A.3),
- A satisfies (A.3) but may not satisfy (A.2).

Then we consider the operator

$$\mathcal{J} := I + A - I \cdot A.$$

Here $I \cdot A$ is interpreted as follows: $(I \cdot A)v = Iw$ where $w \in [\ell(\mathbb{Z}^s)]^{k \times \#A_r}$ consists of the order r Hermite data sampled from the C^r (recall $r' \geq r$) function Iv :

$$w_j(\alpha) = \delta^{\leq r}(Iv)(\alpha + c^j).$$

It is easy to verify that \mathcal{I} satisfies both (A.2) and (A.3), also it is local, linear and shift invariant.

Constructing I : Let h be an order r Hermite interpolant in the sense of [9], i.e. $h = (h_\nu)_{\nu \in A_r}$ consists of component functions which are C^r and compactly supported and satisfy

$$D^\mu h_\nu(\alpha) = \delta_{\mu,\nu} \delta_{\alpha,0}.$$

By (the proof of) [9, Lemma 2.6], h_ν can be chosen to be $C^{r'}$ and supported at $[-1, 1]^s$. Let

$$d := 0.49 \min\{\|c^i - c^j + \alpha\|_\infty : i \neq j, \alpha \in \mathbb{Z}^2\} > 0.$$

Then one can create a Hermite interpolant \bar{h} supported at $[-d, d]^s$ by

$$\bar{h}_\nu := h(\cdot/d)d^{|\nu|}.$$

Define I by

$$Iv := \sum_{\alpha \in \mathbb{Z}^s} \sum_{j=1}^k v^j(\alpha) \bar{h}(\cdot - \alpha - c^j).$$

Notice that the supports of $\bar{h}(\cdot - \alpha - c^j)$ for different α and j are disjoint, therefore I satisfies (A.2). (On the other hand, Iv always vanishes away from the lattice $\bigcup_{1 \leq j \leq k} (\mathbb{Z}^s + c^j)$, so I cannot possibly satisfy (A.3), not even for $l = 1$.)

Constructing A : One way to construct such an A is to construct an operator that interpolates *only* the point values $v^1(\alpha)_0$ in an input Hermite data $v \in [\ell(\mathbb{Z}^s)]^{k \times \#A_r}$. Consider the tensor product polynomial space

$$\Pi_{l-1}(\mathbb{R}^1) \times \cdots \times \Pi_{l-1}(\mathbb{R}^1) := \text{span} \left\{ (\cdot)^\mu : \max_{i=1,\dots,s} \mu_i < l \right\} \supset \Pi_{l-1}(\mathbb{R}^s).$$

For each $\alpha \in \mathbb{Z}^s$, there exists a unique $p_\alpha \in \Pi_k(\mathbb{R}^1) \times \cdots \times \Pi_k(\mathbb{R}^1)$ such that

$$p_\alpha(\alpha + \beta + c^1) = v^1(\alpha + \beta)_0,$$

for β with $0 \leq \beta_i < l$. Pick a compactly supported $C^{r'}$ function N whose shifts form a smooth partition of unity, i.e. $\sum_\alpha N(\cdot - \alpha) = 1$; then the operator A defined by

$$(Av)(x) := \sum_{\alpha \in \mathbb{Z}^s} N(x - \alpha) p_\alpha(x)$$

possesses all the desired properties. \square

Proof of Theorem 3.3. Let ψ be given by Lemma A.1 with

$$k = 2, \quad c^1 = c, \quad c^2 = c', \quad s = 2, \quad l = r + 1, \quad r' = r,$$

then, by comments around (3.9), ψ satisfies moment conditions with respect to a y that satisfies (3.10). Denote by ψ_c and $\psi_{c'}$ the first and last $\#A_r$ components of ψ .

By assumption, \mathbf{a} satisfies sum rules of order $r + 1$ with a y that also satisfies (3.10), and also that $v_\infty(\mathbf{a}, M) > r$, then by Theorem 3.2, we have

$$\lim_{n \rightarrow \infty} \|Q_{\mathbf{a}, M}^n \psi - \phi\|_{[C^r(\mathbb{R}^2)]^{m \times 1}} = 0$$

for some $\phi \in [C^r(\mathbb{R}^2)]^{m \times 1}$; note that ϕ must be a solution of the refinement equation.

Now we show that $S_{\mathbf{a}, M}$ satisfies the Hermite property in Definition (3.1). Let $v \in [\ell^0(\mathbb{Z}^2)]^{1 \times \#A_r}$, and $v_n = S^n v$. We can also write $v_n = \sum_{\beta} v(\beta) \mathbf{a}_n(\cdot - M^n \beta)$ where $\mathbf{a}_n = S^n(\delta I_{m \times m})$, $m = \#A_r$; on the other hand, we have

$$Q^n \psi = \sum_{\alpha \in \mathbb{Z}^2} \mathbf{a}_n(\alpha) \psi(M^n \cdot - \alpha).$$

Then

$$\begin{aligned} f_n &:= \sum_{\alpha \in \mathbb{Z}^2} v_n(\alpha) \psi(M^n \cdot - \alpha) \\ &= \sum_{\alpha \in \mathbb{Z}^2} \sum_{\beta \in \mathbb{Z}^2} v(\beta) \mathbf{a}_n(\alpha - M^n \beta) \psi(M^n \cdot - \alpha) = \sum_{\beta \in \mathbb{Z}^2} v(\beta) (Q^n \psi)(\cdot - \beta). \end{aligned} \tag{A.4}$$

Therefore, if $f := \sum_{\alpha} v(\alpha) \phi(\cdot - \alpha)$, then $\lim_{n \rightarrow \infty} \|f_n - f\|_{C^r(\mathbb{R}^2)} = 0$ and $\lim_{n \rightarrow \infty} \|D^\mu f_n - D^\mu f\|_{L^\infty} = 0$, $\forall \mu \in A_r$.

For a length l column vector of C^r functions f , we denote by $\partial^{\leq r} f(x)$ the $l \times \#A_r$ matrix with the j th row equals to $\partial^{\leq r} f_j$. According to (A.1), for $\alpha \in \mathbb{Z}^2$,

$$\partial^{\leq r} \psi(\alpha + c) = \delta(\alpha) \begin{bmatrix} I_{\#A_r \times \#A_r} \\ 0_{\#A_r \times \#A_r} \end{bmatrix}, \quad \partial^{\leq r} \psi(\alpha + c') = \delta(\alpha) \begin{bmatrix} 0_{\#A_r \times \#A_r} \\ I_{\#A_r \times \#A_r} \end{bmatrix}.$$

Then by (A.4) and (1.2)

$$\begin{aligned} \partial^{\leq r} f_n(M^{-n}(\alpha + c)) &= \sum_{\beta \in \mathbb{Z}^2} v_n(\beta) (\partial^{\leq r} \psi)(\alpha + c - \beta) \mathcal{S}(M^n, A_r) \\ &= v_n^1(\alpha) \mathcal{S}(M^n, A_r). \end{aligned}$$

It follows that

$$\begin{aligned} &\max_{\alpha \in \mathbb{Z}^2} \|\partial^{\leq r} f(M^{-n}(\alpha + c)) - v_n^1(\alpha) \mathcal{S}(M^n, A_r)\|_\infty \\ &= \max_{\alpha \in \mathbb{Z}^2} \|\partial^{\leq r} f(M^{-n}(\alpha + c)) - \partial^{\leq r} f_n(M^{-n}(\alpha + c))\|_\infty \\ &\leq \max_{\mu \in A_r} \|D^\mu f_n - D^\mu f\|_{L^\infty} \rightarrow 0, \quad \text{as } n \rightarrow \infty. \end{aligned}$$

Since $f \in [C^r(\mathbb{R}^2)]^{m \times 1}$,

$$\begin{aligned} &\|\partial^{\leq r} f(M^{-n} \alpha) - v_n^1(\alpha) \mathcal{S}(M^n, A_r)\|_\infty \\ &\leq \|\partial^{\leq r} f(M^{-n} \alpha) - \partial^{\leq r} f(M^{-n}(\alpha + c))\|_\infty + \|\partial^{\leq r} f(M^{-n}(\alpha + c)) - v_n^1(\alpha) \mathcal{S}(M^n, A_r)\|_\infty \\ &\rightarrow 0 + 0, \quad \text{as } n \rightarrow \infty. \end{aligned}$$

Similarly, we can show that

$$\|\partial^{\leq r} f(M^{-n}\alpha) - v_n^2(\alpha)\mathcal{S}(M^n, A_r)\|_\infty \rightarrow 0, \quad \text{as } n \rightarrow \infty.$$

Therefore, the conditions (3.1) and (3.2) in definition (3.1) are satisfied.

The condition $v_\infty(\mathbf{a}, M) > r$ implies that $\text{span}\{\phi(\cdot - \beta) : \beta \in \mathbb{Z}^2\} \supseteq \Pi_r$, which implies $\phi \neq 0$. Thus condition (ii) of Definition (3.1) is also satisfied by \mathbf{a} . \square

Appendix B. Proof of Theorem 4.2

Proof. We first prove that condition (i) implies that $S_{\mathbf{a},M}$ is the symmetry condition in Definition 4.1.

Let $v_0 = H_M^0(f)$ and $w_0 = H_M^0(g)$, where $f \in C^r(\mathbb{R}^2)$, $g = f(E\cdot)$ and $E \in G$. If

$$v_n = S_{a,M}^n v_0, \quad w_n = S_{a,M}^n w_0, \quad n = 1, 2, \dots,$$

then by condition (i), we have

$$w_n = T_E^n v_n \quad \text{for } n = 0, 1, 2, \dots \tag{B.1}$$

For notational convenience, we define the (scalar) sequences $\bar{v}_n^\sigma, \bar{w}_n^\sigma$ by

$$\bar{v}_n^\sigma(\alpha) = (v_n^\sigma(\alpha))_1, \quad \bar{w}_n^\sigma(\alpha) = (w_n^\sigma(\alpha))_1.$$

Definition 3.1 implies in particular that there exist $f_v, f_w \in C^r(\mathbb{R}^2)$ such that

$$\begin{aligned} \lim_{n \rightarrow \infty} \max_{\alpha \in \mathbb{Z}^2} |f_v(M^{-n}\alpha) - \bar{v}_n^\sigma(\alpha)| &= 0, \\ \lim_{n \rightarrow \infty} \max_{\alpha \in \mathbb{Z}^2} |f_w(M^{-n}\alpha) - \bar{w}_n^\sigma(\alpha)| &= 0, \quad \sigma = 1, 2. \end{aligned}$$

It suffices to prove $f_v(E\cdot) = f_w$.

It implies that, for any $\varepsilon > 0$, there exists an $N_1(\varepsilon) > 0$ such that

$$\max_{\alpha \in \mathbb{Z}^2} |f_v(M^{-n}\alpha) - \bar{v}_n^\sigma(\alpha)| < \varepsilon/3 \quad \text{and} \quad \max_{\alpha \in \mathbb{Z}^2} |f_w(M^{-n}\alpha) - \bar{w}_n^\sigma(\alpha)| < \varepsilon/3 \tag{B.2}$$

for any $n \geq N_1(\varepsilon)$, $\sigma = 1, 2$.

Since $f \in C^r(\mathbb{R}^2)$, there exists an $N_2(\varepsilon) > 0$ such that for any $n \geq N_2(\varepsilon)$, $\sigma \in \{1, 2\}$,

$$\max_{\alpha \in \mathbb{Z}^2} |\bar{v}_n^\sigma(\alpha) - \bar{v}_n^\sigma(\alpha + \alpha')| < \varepsilon/3, \quad \text{whenever } \|\alpha'\|_\infty \leq 1. \tag{B.3}$$

Condition (4.5) implies that $M^l E M^{-l} \in G$ for all $l \geq 0$. But G is finite, so there must exist $l \neq l'$ such that $M^l E M^{-l} = M^{l'} E M^{-l'}$, which is the same as saying that there exists an integer $l > 0$ such that $M^l E M^{-l} = E$; this, in turn, implies that

$$M^{kl} E M^{-kl} = E, \quad \forall k \in \mathbb{Z}. \tag{B.4}$$

Now let $\alpha \in \mathbb{Z}^2$, $n \in \{k \cdot l : k = 0, 1, 2, \dots\}$, be arbitrary but fixed. Choose an integer $N \geq \max\{N_1(\varepsilon), N_2(\varepsilon), n\}$ which is also a multiple of l .

So, by (B.4), $M^N E M^{-N} = E$. Then, by (B.1) and (4.7),

$$\bar{w}_N^1(\alpha) = \begin{cases} \bar{v}_N^1(\lfloor E\alpha + E\mathbf{c}^1 \rfloor), & \text{if } E \in D_6^1, \\ \bar{v}_N^2(\lfloor E\alpha + E\mathbf{c}^2 \rfloor), & \text{if } E \in D_6^2. \end{cases}$$

In any case, there exist $\sigma = \sigma(E) \in \{1, 2\}$ and $\alpha' = \alpha'(E, \alpha) \in \mathbb{Z}^2$ with $\|\alpha'\|_\infty \leq 1$ such that

$$\bar{w}_N^1(\alpha) = \bar{v}_N^\sigma(E\alpha + \alpha'). \quad (\text{B.5})$$

Then, writing $\beta := M^{N-n}\alpha$, we have

$$\begin{aligned} |f_v(EM^{-n}\alpha) - f_w(M^{-n}\alpha)| &= |f_v(EM^{-N}M^{N-n}\alpha) - f_w(M^{-N}M^{N-n}\alpha)| \\ &= |f_v(M^{-N}(E\beta)) - f_w(M^{-N}\beta)| \quad (\text{by (B.4)}) \\ &\leq T_1 + T_2 + T_3, \end{aligned}$$

where

$$\begin{aligned} T_1 &:= |f_v(M^{-N}(E\beta)) - \bar{v}_N^\sigma(E\beta)| < \varepsilon/3, \quad T_2 := |f_w(M^{-N}\beta) - \bar{w}_N^1(\beta)| < \varepsilon/3, \text{ and} \\ T_3 &:= |\bar{v}_N^\sigma(E\beta) - \bar{w}_N^1(\beta)| \\ &= |\bar{v}_N^\sigma(E\beta) - \bar{v}_N^\sigma(E\beta + \beta')| \quad \text{for some } \beta' \in \mathbb{Z}^2 \text{ with } \|\beta'\|_\infty \leq 1 \quad (\text{by (B.5)}) \\ &< \varepsilon/3 \quad (\text{by (B.3)}). \end{aligned}$$

Since $\varepsilon > 0$ is arbitrary,

$$f_v(EM^{-n}\alpha) = f_w(M^{-n}\alpha). \quad (\text{B.6})$$

Since the continuous functions $f_v(E\cdot)$ and f_w agree in values on the following dense set of \mathbb{R}^2

$$\{M^{-n}\alpha : \alpha \in \mathbb{Z}^2, n = 1, 2l, 3l, \dots\},$$

they must be the same everywhere. Therefore, $S_{\mathbf{a},M}$ is a G -symmetric honeycomb Hermite subdivision operator.

It is obvious that (i) \Rightarrow (ii) \Rightarrow (iii), so to finish the proof of the theorem it suffices to show (ii) \Rightarrow (i) and (iii) \Rightarrow (ii).

(ii) \Rightarrow (i): By (4.6) and the chain rule (1.2), we have, for any smooth function f ,

$$H_M^n(f) = H_M^{n-1}(f(M^{-1}\cdot));$$

this combined with the definition of T_E^n (4.6) yields

$$T_E^n = T_{M^{-1}EM}^{n-1}, \quad n = 1, 2, 3, \dots$$

Suppose we have $S_{\mathbf{a},M} \circ T_E^0 = T_E^1 \circ S_{\mathbf{a},M}$, then

$$S_{\mathbf{a},M} \circ T_E^1 = S_{\mathbf{a},M} \circ T_{M^{-1}EM}^0 = T_{M^{-1}EM}^1 \circ S_{\mathbf{a},M} = T_E^2 \circ S_{\mathbf{a},M}.$$

Then one can proceed by induction to prove (i).

(Notice the important role played by the compatibility condition (4.4) in the argument above.)

(iii) \Rightarrow (ii): Observe the following properties of T_E^n and $S := S_{a,M}$: for any $\alpha \in \mathbb{Z}^2$

$$T_E^n(v(\cdot - \alpha)) = (T_E^n v)(\cdot - M^n E^{-1} M^{-n} \alpha), \quad (\text{B.7})$$

$$S(v(\cdot - \alpha)) = (Sv)(\cdot - M\alpha). \quad (\text{B.8})$$

Denote by w_j the sequence δe_j^T , where $j \in \{1, \dots, m\}$. Since both S and T_E^n are linear and local operators, it suffices to prove

$$(T_E^1 \circ S)(w_j(\cdot - \alpha)) = (S \circ T_E^0)(w_j(\cdot - \alpha)), \quad \forall \alpha \in \mathbb{Z}^2, \quad j \in \{1, \dots, m\}. \quad (\text{B.9})$$

But we have

$$\begin{aligned} (T_E^1 \circ S)(w_j(\cdot - \alpha)) &\stackrel{(\text{B.8})}{=} T_E^1((S w_j)(\cdot - M\alpha)) \stackrel{(\text{B.7})}{=} (T_E^1(S w_j))(\cdot - M E^{-1} M^{-1} M\alpha) \\ (S \circ T_E^0)(w_j(\cdot - \alpha)) &\stackrel{(\text{B.7})}{=} S((T_E^0(w_j))(\cdot - E^{-1}\alpha)) \stackrel{(\text{B.8})}{=} (S(T_E^0 w_j))(\cdot - M E^{-1}\alpha). \end{aligned}$$

Then by (iii), (B.9) holds. \square

References

- [1] R.E. Barnhill, J.A. Gregory, Polynomial interpolation to boundary data on triangles, *Math. Comput.* 29 (131) (1975) 726–735.
- [2] W. Boehm, H. Prautasch, Box spline, in: G. Farin, J. Hoschek, M.-S. Kim (Eds.), *Handbook of Computer Aided Geometric Design*, Elsevier, Amsterdam, 2002, pp. 255–282 (Chapter 10).
- [3] J. Claes, K. Beets, F. Van Reeth, A corner-cutting scheme for hexagonal subdivision surfaces, in: *Proceedings of the International Conference on Shape Modeling and Applications (SMI '02)*, 2002, pp. 13–20.
- [4] B. Han, Approximation properties and construction of Hermite interpolants and biorthogonal multiwavelets, *J. Approx. Theory* 110 (1) (2001) 18–53.
- [5] B. Han, Vector cascade algorithms and refinable function vectors in Sobolev spaces, *J. Approx. Theory* 124 (1) (2003) 44–88.
- [6] B. Han, Classification and construction of bivariate subdivision schemes, in: J.-L. Merrien, A. Cohen, L.L. Schumaker (Eds.), *Proceeding on Curves and Surfaces Fitting: Saint-Malo 2002*, 2003, pp. 187–197.
- [7] B. Han, M. Overton, T.P.-Y. Yu, Design of Hermite subdivision schemes aided by spectral radius optimization, *SIAM J. Sci. Comput.* 25 (2) (2003) 643–656.
- [8] B. Han, T.P.-Y. Yu, Face-based Hermite subdivision schemes, *J. Concrete Appl. Math.*, preprint available at <http://www.rpi.edu/~yut/Papers/dual.pdf>, 2003, to appear in special issue in *Wavelets, Statistics and Applications*.
- [9] B. Han, T.P.-Y. Yu, B. Piper, Multivariate refinable Hermite interpolants, *Math. Comput.* 73 (248) (2004) 1913–1935.
- [10] B. Han, T.P.-Y. Yu, Y. Xue, Non-interpolatory Hermite subdivision schemes, *Math. Comput.*, posted on September 10, 2004, PII S 0025-5718(00)01244-8, to appear.
- [11] R.Q. Jia, Q.T. Jiang, Spectral analysis of the transition operator and its applications to smoothness analysis of wavelets, *SIAM J. Matrix Anal. Appl.* 24 (4) (2003) 1071–1109.
- [12] Q. Jiang, P. Oswald, Triangular $\sqrt{3}$ -subdivision schemes: the regular case, *J. Comput. Appl. Math.* 156 (1) (2003) 47–75.
- [13] N.S. Sapidis, *Designing Fair Curves and Surfaces: Shape Quality in Geometric Modeling and Computer-aided Design*, SIAM, Philadelphia, PA, 1994.
- [14] Y. Xue, T.P.-Y. Yu, Jet subdivision scheme on k -regular complex, preprint available at <http://www.rpi.edu/~yut/Papers/JSSOKRC.pdf>, September 2004, submitted for publication.
- [15] Y. Xue, T.P.-Y. Yu, T. Duchamp, Jet subdivision surfaces: applications of vector refinability to free-form surfaces, 2004 in preparation.